MAGNETIC COUPLINGS WITH CYLINDRICAL AND PLANE AIR GAPS: INFLUENCE OF THE MAGNET POLARIZATION DIRECTION

R. Ravaud and G. Lemarquand

Laboratoire d'Acoustique de l'Universite du Maine
UMR CNRS 6613, Avenue Olivier Messiaen, Le Mans 72085, France

Abstract—This paper presents a comparison of cylindrical and plane air gap magnetic couplings in which the tile permanent magnet polarizations can be either radial or tangential or axial. The expressions of the torque transmitted between the two rotors of each coupling are determined by using the colombian approach. All the calculations are performed without any simplifying assumptions. Consequently, the expressions obtained are accurate and enable a fast comparison between the structures presented in this paper.

1. INTRODUCTION

Magnetic couplings are devices that allow the transmission of torque without contact. They have been studied for many years but the new rare earth permanent magnet materials give them a real development [1–11]. Furthermore, these contactless structures enable the torque transmission through a dividing wall. Besides, this wall can be either a plane or a cylinder and so the airgap type determines two couplings families. Moreover, the study of magnetic couplings relies on the analytical expressions of the magnetic field created by permanent magnets of various shapes [12–16], and especially parallelepipeds [17, 18], tiles [19–22], rings [23, 24] and cylinders [25, 26]. The first analytical formulations for the forces between cuboidal magnets was given by Akoun and Yonnet [27]. Then, these expressions were completed for various shapes and this allowed the design and optimization of couplings devoted to different applications [28–34]. Furthermore, one should remark that the calculation of the forces between magnets is analogous to

---

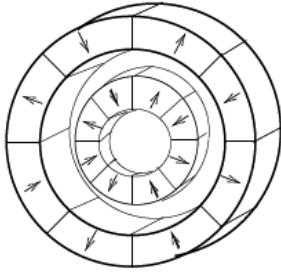Corresponding author: G. Lemarquand (guy.lemarquand@univ-lemans.fr).

Figure 1. Magnetic coupling using a cylindrical air gap and tile permanent magnets radially magnetized.
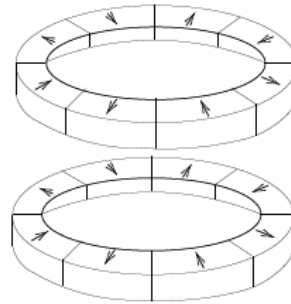
Figure 2. Magnetic coupling using a plane gap and tile permanent magnets radially magnetized.

the calculation of the mutual inductance of two current carrying coils [35, 36]. Some authors also study magnetic couplings with finite elements calculations [37, 39].

The main configurations generaly used for realizing magnetic couplings are presented below. Indeed, magnetic couplings are built with either cylindrical air gaps, as shown in Fig. 1, or with plane air gaps, as shown in Fig. 2.

Some analytical studies have been performed by several authors [27–40] for studying such magnetic couplings. However, these studies omitted the curvature effect of the tile permanent magnets. On the other hand, such approaches, based on the linearized model of a magnet, are fully analytical and thus interesting to use for optimization purposes.

We propose in this paper to use an exact formulation based on the coulombian model for calculating the torque transmitted bewteen tile permanent magnets radially, tangentially or axially magnetized. Our semi-analytical expressions are based on a single numerical integration whose convergence is fast and robust. All the analytical expressions have been determined without any simplifying assumptions.

2. CONFIGURATIONS STUDIED IN THIS PAPER

We present in this section the six configurations studied in this paper. Strictly speaking, our investigation encompasses both the classical magnetic couplings but also unconventional couplings manufactured with tile permanent magnets tangentially magnetized. The choice of the tile permanent magnet polarization depends greatly on the involved

application. Basically, the main criterion for optimizing magnetic couplings is the value of the torque transmitted between the two rotors. To do so, several criteria must be taken into account: the media used, the number and the tile dimensions as well as the intrinsic properties of the magnets (coercitive field). However, the shape of the torque versus the angular shift can also be the main optimization criterion. This is why several configurations of tile permanent magnets with different polarizations must be compared to each other. We have represented in Fig. 3 three magnetic couplings using only cylindrical air gaps.

The three magnetic couplings presented in Fig. 3 are composed of tile permanent magnets radially, tangentially or axially magnetized. Magnetic couplings using tile permanent magnets radially or axially magnetized are rather well known whereas the ones using tile permanent magnets tangentially magnetized are less known. The magnetic couplings using plane air gaps are presented in Fig. 4. The three magnetic couplings presented in Fig. 4 are also composed of tile permanent magnets radially, tangentially and axially magnetized. Such couplings are used in pharmaceutical processes.
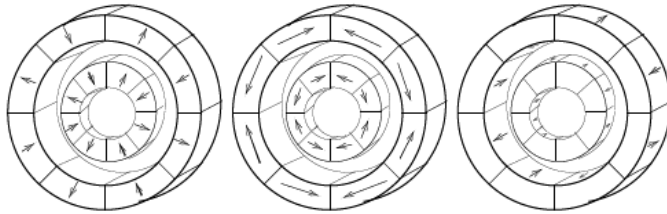

Figure 3. Magnetic couplings using cylindrical air gaps; from left to right: coupling using tile permanent magnets radially magnetized, coupling using tile permanent magnets tangentially magnetized, coupling using tile permanent magnets axially magnetized.

Figure 4. Magnetic couplings using plane air gaps; from left to right: coupling using tile permanent magnets radially magnetized, coupling using tile permanent magnets tangentially magnetized, coupling using tile permanent magnets axially magnetized.
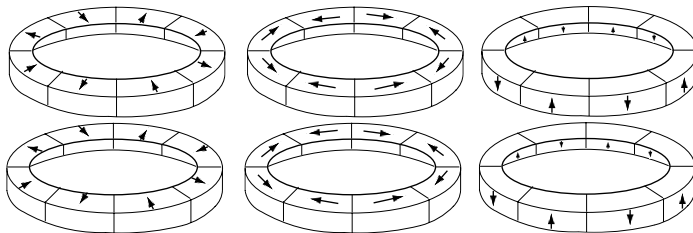
3. STUDY WITH THE COLOMBIAN MODEL FOR STUDYING THE MAGNETIC COUPLINGS

We present now the three-dimensional equations for the study of the structures presented in the previous section.

3.1. Torque Transmitted between Two Tile Permanent Magnets Radially Magnetized

The torque transmitted between two tile permanent magnets radially magnetized is determined by using the analytical expressions determined in a previous paper [20]. These analytical expressions are based on the colombian model of a magnet.

3.2. Torque Transmitted between Two Tile Permanent Magnets Tangentially Magnetized

Let us now consider the torque transmitted between two tile permanent magnets tangentially magnetized. The geometry considered and the related parameters are shown in Fig. 5. All the calculations are carried out by using the coulombian model. Thus, each tile permanent magnet is represented by magnetic pole surface densities that appear only on the straight faces of the each tile (Fig. 5). For the tile located on the left in Fig. 5, its inner radius is r_1 and its outer one is r_2. Its angular width is $\theta_2 - \theta_1$ and its height is $z_2 - z_1$. Its magnetic polarization $\vec{J}_1$ is directed along $\vec{u}_\theta$ in cylindrical coordinates. For the tile located on the left in Fig. 5, its inner radius is r_3 and its outer one is r_4. Its angular width is $\theta_4 - \theta_3$ and its height is $z_4 - z_3$. Its magnetic polarization $\vec{J}_2$ is directed along $\vec{u}_\theta$ in cylindrical coordinates. The torque transmitted between the two tile permanent magnets tangentially magnetized is determined by integrating the magnetic field produced by the inner
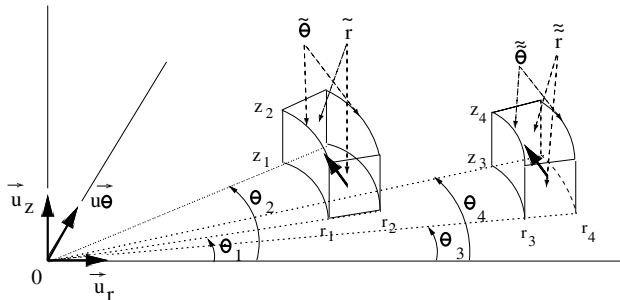

Figure 5. Two tile permanent magnets tangentially magnetized.

tile permanent magnet on the magnetic pole surface densities of the outer tile permanent magnet. By denoting $\mathbf{H}(r, \theta, z)$, the magnetic field produced by the inner tile permanent magnet in all points in space, the torque transmitted bewteen the two tile permanent magnets can be expressed as follows:

$$
\begin{aligned}
T = \; & J_2 \int_{r_3}^{r_4} \int_{z_1}^{z_2} H_\theta \left(\tilde{r}, \theta_4, \tilde{z} \right) \tilde{r} d\tilde{r} d\tilde{z} \\
& - J_2 \int_{r_3}^{r_4} \int_{z_1}^{z_2} H_\theta \left(\tilde{r}, \theta_3, \tilde{z} \right) \tilde{r} d\tilde{r} d\tilde{z}
\end{aligned}
\tag{1}
$$

where $H_\theta(r, \theta, z)$ is expressed as follows:

$$
H_\theta(r, \theta, z) = -\vec{\nabla} \cdot \left(\int_{r_1}^{r_2} \int_{z_1}^{z_2} G\left(\vec{r}, \vec{r'} \right) d\phi \left(\vec{r'} \right) \right) \cdot \vec{u}_\theta
\tag{2}
$$

where $G(\vec{r}, \vec{r'})$ is the three-dimensional Green's function defined as follows:

$$
G\left(\vec{r}, \vec{r'} \right) = \frac{1}{4\pi \left| \vec{r} - \vec{r'} \right|}
\tag{3}
$$

where $\vec{r}$ an observation point and $\vec{r'}$ a point located on the charge distribution. It is noted that $G(\vec{r}, \vec{r'})$ has been largely used in [19]. In addition, $d\phi(\vec{r'})$ is defined by :

$$
d\phi \left(\vec{r'} \right) = \frac{J_1}{\mu_0} d\tilde{r} d\tilde{z}
\tag{4}
$$

By setting $x = \cos(\theta_m - \theta_j)$, $y = \sin(\theta_m - \theta_j)$ and $c = r_i^2 + (z_n - z_k)^2$, the final expression of the torque can be written as follows:

$$
T = \sum_{i,j,k,m,n=1}^{2} (-1)^{(i+j+k+m+n)} \int_{r_3}^{r_4} \vartheta \left(\tilde{r}, i, j, k, m, n \right) d\tilde{r}
\tag{5}
$$

and $\vartheta \left(\tilde{r}, i, j, k, m, n \right)$ is expressed as follows:

$$
\begin{aligned}
\vartheta \left(\tilde{r}, i, j, k, m, n \right) = \; & \tilde{r} y \sqrt{ \tilde{r}^2 + (z_k - z_n)^2 + r_i \left(r_i - 2\tilde{r}x \right) } \\
& + \tilde{r} x \log \left[r_i - \tilde{r}x + \sqrt{ \tilde{r}^2 + (z_k - z_n)^2 + r_i^2 - 2r_i \tilde{r}x } \right] \\
& - \frac{(z_k - z_n) \left(\sqrt{x^2 - 1} - x \right)}{2\sqrt{x^2 - 1}} \log[A_{i,j,k,m,n}]
\end{aligned}
$$

$$-\frac{(z_k-z_n)\left(\sqrt{x^2-1}+x\right)}{2\sqrt{x^2-1}}\log[B_{i,j,k,m,n}] \tag{6}$$

$$A_{i,j,k,m,n}=\frac{-2}{(z_k-z_n)^3}\frac{\left(r_i\tilde{\tilde{r}}(x^2-1)-\xi+\tilde{\tilde{r}}^2(x^2-1)\left(\sqrt{x^2-1}-x\right)\right)}{\left(\sqrt{x^2-1}-x\right)\left(r_i+\tilde{\tilde{r}}\left(\sqrt{x^2-1}-x\right)\right)}$$

$$B_{i,j,k,m,n}=\frac{-2}{(z_k-z_n)^3}\frac{\left(r_i\tilde{\tilde{r}}(x^2-1)+\xi-\tilde{\tilde{r}}^2(x^2-1)\left(\sqrt{x^2-1}+x\right)\right)}{\left(\sqrt{x^2-1}-x\right)\left(-r_i+\tilde{\tilde{r}}\left(\sqrt{x^2-1}+x\right)\right)} \tag{7}$$

$$\xi=\sqrt{x^2-1}(z_k-z_n)\left(z_k-z_n+\sqrt{r_i^2+\tilde{\tilde{r}}^2-2r_i\tilde{\tilde{r}}x+(z_k-z_n)^2}\right)$$

3.3. Torque Transmitted between Two Tile Permanent Magnets Axially Magnetized

The torque transmitted between the two tile permanent magnets axially magnetized is determined by integrating the magnetic field produced by the inner tile permanent magnet on the magnetic pole surface densities of the outer tile permanent magnet. By denoting $\mathbf{H}(r,\theta,z)$, the magnetic field produced by the inner tile permanent magnet in all points in space, the torque transmitted between the two tile permanent magnets can be expressed as follows:

$$T = J_2\int_{r_3}^{r_4}\int_{\theta_3}^{\theta_3}H_\theta\left(\tilde{\tilde{r}},\tilde{\tilde{\theta}},z_2\right)\tilde{\tilde{r}}d\tilde{\tilde{r}}d\tilde{\tilde{\theta}}$$

$$-J_2\int_{r_3}^{r_4}\int_{\theta_3}^{\theta_4}H_\theta\left(\tilde{\tilde{r}},\tilde{\tilde{\theta}},z_1\right)\tilde{\tilde{r}}d\tilde{\tilde{r}}d\tilde{\tilde{\theta}} \tag{8}$$
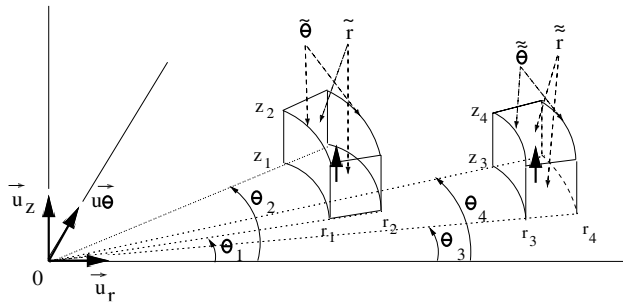

Figure 6. Two tile permanent magnets axially magnetized.

where $H_\theta(r, \theta, z)$ is expressed as follows:

$$H_\theta(r, \theta, z) = -\vec{\nabla} \cdot \left(\int_{r_1}^{r_2} \int_{\theta_1}^{\theta_2} G\left(\vec{r}, \vec{r'}\right) d\phi\left(\vec{r'}\right) \right) \cdot \vec{u}_\theta \qquad (9)$$

where

$$d\phi\left(\vec{r'}\right) = \frac{J_1}{\mu_0} \tilde{r} d\tilde{r} d\tilde{\theta} \qquad (10)$$

By setting $\xi = \sqrt{r_i^2 + r_l^2 - 2 r_i r_l x + (z_n - z_k)^2}$ and $\xi_2 = \xi + r_l - r_i x$, the expression of the torque transmitted between two tile permanent magnets axially magnetized can be written as follows:

$$T = \sum_{i,j,k,l,n=1}^{2} (-1)^{(i+j+k+l+n)} \int_{\theta_3}^{\theta_4} \vartheta\left(\tilde{\tilde{\theta}}, i, j, k, l, n\right) d\tilde{\tilde{\theta}} \qquad (11)$$

$$\vartheta\left(\tilde{\tilde{\theta}}, i, j, k, l, n\right) = \frac{b^{\frac{3}{2}} x}{3 (x^2-1)^{\frac{3}{2}}} \tanh^{-1}\left[\frac{r_l \sqrt{x^2-1}}{\sqrt{b}}\right] - \frac{r_l^3 x}{9} - \frac{b r_l x}{3 (x^2-1)}$$

$$+ \frac{x \xi}{6 (x^2-1)} \left(-r_i r_l - 2bx - 3 r_i^2 x + r_i r_l x^2 + 3 r_i^2 x^3\right)$$

$$+ x \log(\xi_2) \left(-\frac{b r_i}{2} + \frac{r_i^3 x^2}{2} + \frac{r_i^3}{6}\right)$$

$$+ \frac{\xi}{6} \left(-r_i r_l x + r_i^2 \left(2 - 3x^2\right) + 2 \left(r_l^2 + (z_n - z_k)^2\right)\right)$$

$$- \frac{\log(\xi_2)}{2} \left(r_i x \left(r_i^2 \left(x^2 - 1\right) - (z_n - z_k)^2\right)\right)$$

$$+ \frac{\left(b^{\frac{3}{2}} r_i x - b^{\frac{3}{2}} r_i x^3 + b^2 x^2\right) \log\left(A^I\right)}{6 (x^2-1)^{\frac{3}{2}} \sqrt{b x^2 - 2\sqrt{b} r_i x \sqrt{x^2-1} + r_i^2 (x^2-1)}}$$

$$+ \frac{\left(-b^{\frac{3}{2}} r_i x + b^{\frac{3}{2}} r_i x^3 + b^2 x^2\right) \log\left(A^{II}\right)}{6 (x^2-1)^{\frac{3}{2}} \sqrt{b x^2 + 2\sqrt{b} r_i x \sqrt{x^2-1} + r_i^2 (x^2-1)}} \qquad (12)$$

By setting $\alpha^{+,-} = \sqrt{b x^2 \pm 2\sqrt{b} r_i x \sqrt{x^2 - 1} + r_i^2 (x^2 - 1)}$, the parameters A^I and A^{II} are defined as follows:

$$A^I = \frac{6 \left(x^2-1\right)^2 \left(-r_i^2 + r_i r_l x + r_i^2 x^2 - r_i r_l x^3\right)}{b^{\frac{3}{2}} \left(r_l - r_l x^2 + \sqrt{b} \sqrt{x^2-1}\right) \alpha^- \left(r_i - r_i x^2 + \sqrt{b} x \sqrt{x^2-1}\right)}$$

$$+\frac{6\left(x^2-1\right)^2\left(\sqrt{b}\left(r_l-r_ix\right)\sqrt{x^2-1}+b\left(x^2-1\right)+\xi\sqrt{x^2-1}\alpha^-\right)}{b^{\frac{3}{2}}\left(r_l-r_lx^2+\sqrt{b}\sqrt{x^2-1}\right)\alpha^-\left(r_i-r_ix^2+\sqrt{b}x\sqrt{x^2-1}\right)} \quad (13)$$

$$A^{II}=\frac{6\left(x^2-1\right)^2\left(b+r_i^2-r_ir_lx-bx^2-r_i^2x^2+r_ir_lx^3\right)}{b^{\frac{3}{2}}\left(\sqrt{b}x\sqrt{x^2-1}+r_i\left(x^2-1\right)\right)\alpha^+\left(\sqrt{b}\sqrt{x^2-1}+r_l\left(x^2-1\right)\right)}$$

$$+\frac{6\left(x^2-1\right)^2\left(\sqrt{b}\left(r_l-r_ix\right)\sqrt{x^2-1}-\xi\sqrt{x^2-1}\alpha^+\right)}{b^{\frac{3}{2}}\left(\sqrt{b}x\sqrt{x^2-1}+r_i\left(x^2-1\right)\right)\alpha^+\left(\sqrt{b}\sqrt{x^2-1}+r_l\left(x^2-1\right)\right)} \quad (14)$$

4. COMPARISON OF THREE KINDS OF MAGNETIC COUPLINGS WITH A CYLINDRICAL AIR GAP

This section presents a comparison between three kinds of magnetic couplings using cylindrical air gaps. The torque transmitted between the outer (led rotor) and inner (leading rotor) rotors is determined for three configurations using 8, 16 and 32 tile permanent magnets. In other words, the angular widths of each tile permanent magnet are $\frac{\pi}{4}$ rad, $\frac{\pi}{8}$ rad, $\frac{\pi}{16}$ rad, $\frac{\pi}{32}$ rad and $\frac{\pi}{64}$ rad. For each tile permanent magnet, we have $r_1 = 0.0219\,\text{m}$, $r_2 = 0.0249\,\text{m}$, $r_3 = 0.025\,\text{m}$, $r_4 = 0.028\,\text{m}$, $z_1 = 0\,\text{m}$, $z_2 = 0.003\,\text{m}$, $z_3 = 0\,\text{m}$, $z_4 = 0.003\,\text{m}$. For the rest of this paper, all the simulations have been carried out with 2 tile permanent magnets on each rotor.

4.1. Simulations

The simulations have been carried out with the following dimensions: each tile permanent magnet has a magnetic polarization that equals 1 T. Their radial width is 3 mm and their height is 3 mm. The air gap between the two rotors is 0.1 mm. The torque transmitted between the two rotors is represented versus the angle θ, that is, versus the angular shift between the two rotors.

4.2. Discussion

Figure 7 shows that tile permanent magnets radially magnetized are the best solution for having the greatest torque between two rotors with a cylindrical air gap. However, as tile permanent magnets radially magnetized are rather difficult to manufacture, it can be interesting to compare the torque transmitted between two rotors made of tile

permanent magnets tangentially magnetized and two rotors made of tile permanent magnets axially magnetized. Fig. 7 shows that tile permanent magnets tangentially magnetized are required when the number of tile permanent magnets used is high (typically superior to 32 for each rotor). When this number is lower, it is more interesting to use tile permanent magnets axially magnetized.
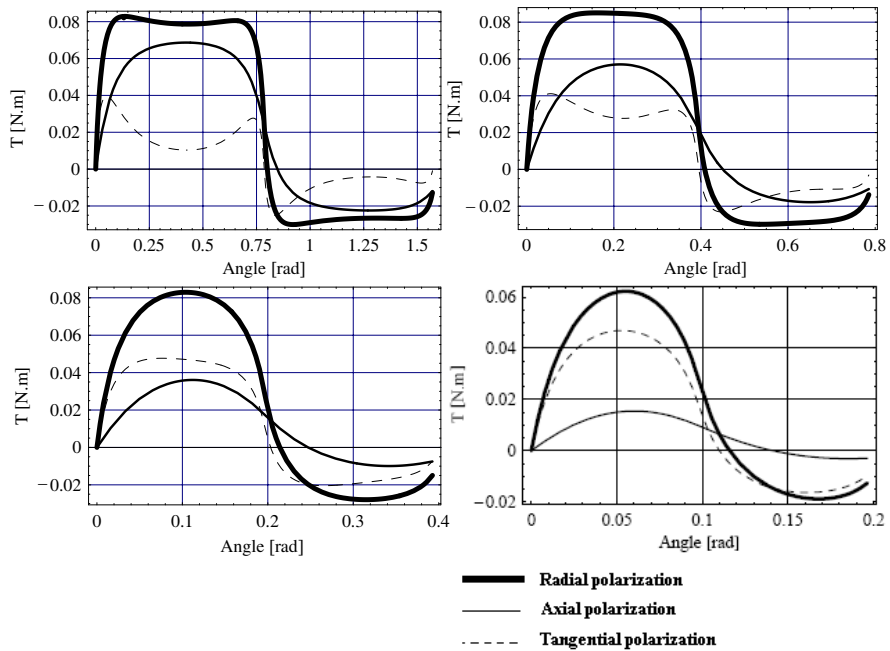

Figure 7. Representation of the torque transmitted between two rotors with a cylindrical air gap with tile permanent magnets radially, tangentially and axially magnetized. The angular widths taken are $\frac{\pi}{4}$ rad, $\frac{\pi}{8}$ rad, $\frac{\pi}{16}$ rad and $\frac{\pi}{32}$ rad respectively from the upper figure to the lower figure.

5. COMPARISON OF THREE KINDS OF MAGNETIC COUPLINGS USING A PLANE AIR GAP

5.1. Simulations

The simulations have been carried out with the following dimensions: each tile permanent magnet has a magnetic polarization that equals 1 T. Their radial width is 3 mm and their height is 3 mm. The air gap
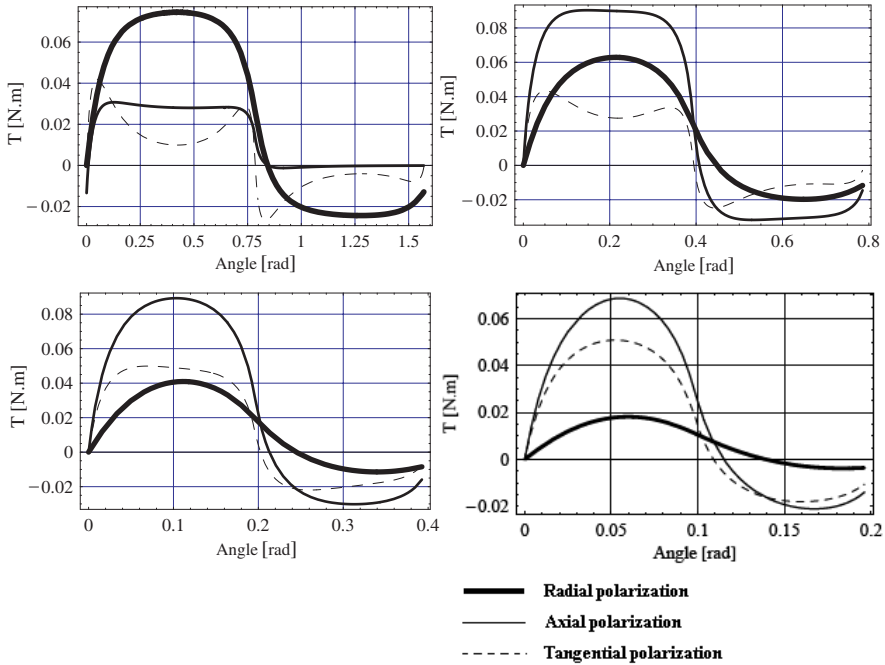
Figure 8. Representation of the torque transmitted between two rotors with a plane air gap with tile permanent magnets radially, tangentially and axially magnetized. The angular widths taken are $\frac{\pi}{4}$ rad, $\frac{\pi}{8}$ rad, $\frac{\pi}{16}$ rad and $\frac{\pi}{32}$ rad respectively from the upper figure to the lower figure.

between the two rotors is 0.1 mm. For each tile permanent magnet, we have $r_1 = 0.025$ m, $r_2 = 0.028$ m, $r_3 = 0.025$ m, $r_4 = 0.028$ m, $z_1 = 0.0031$ m, $z_2 = 0.0061$ m, $z_3 = 0$ m, $z_4 = 0.003$ m.

6. PARAMETRIC STUDY OF THE TORQUE TRANSMITTED IN CYLINDRICAL AIR GAPS USING TILE PERMANENT MAGNETS RADIALLY, AXIALLY AND TANGENTIALLY MAGNETIZED

6.1. Couplings Using Cylindrical Air Gaps

We present in this section a parametric study of the torque transmitted between the stator and the rotor of a coupling made of two tile permanent magnets with radial, axial or tangential polarizations

located on the led and leading parts of this device. For this purpose, we consider first a coupling using a cylindrical air gap with the following dimensions: $r_2 - r_1 = 0.003\,\text{m}$, $r_4 - r_3 = 0.003\,\text{m}$, $z_1 = 0\,\text{m}$, $z_2 = 0.003\,\text{m}$, $z_3 = 0\,\text{m}$, $z_4 = 0.003\,\text{m}$, $J_1 = J_2 = 1\,\text{T}$, $\theta_4 - \theta_3 = \theta_2 - \theta_1 = \frac{\pi}{32}$.

We represent in Figs. 9(a)–(c) the torque transmitted between the leading and led parts of a coupling for four air gaps ($0.1\,\text{mm}$, $0.3\,\text{mm}$, $0.5\,\text{mm}$, $1\,\text{mm}$). In the three configurations, the smallest the air gap is, the greatest the torque is. These figures also show that the way the torque decreases versus both the angular shift and the air gap is similar for the three polarizations of the tile permanent magnets. The other important parameter that can be optimized in a magnetic coupling is certainly the thickness of the permanent magnets on each parts. We represent in Figs. 10(a)–(c) the torque transmitted between the leading and led parts of a coupling for three magnet thicknesses ($0.003\,\text{m}$, $0.005\,\text{m}$, $0.011\,\text{m}$). In the three configurations, the smallest the magnet thickness is, the greatest the torque is. These figures also show that the way the torque decreases versus both the angular shift and the air gap is similar for the three polarizations of the tile permanent magnets. In short, the previous figures show that for a cylindrical coupling, the air gap must be the smallest and the magnet thickness must be the greatest and the magnet polarization should be radial.

We can apply the previous results to the case of plane magnetic couplings. Indeed, in the case of plane air gaps, the air gap must also be the smallest, the magnet height must be the greatest and the magnet polarization should be axial.

6.2. Discussion

Figure 8 shows that tile permanent magnets axially magnetized are not always the best solution for having the greatest torque between two rotors with a plane air gap. When the number of tile permanent magnets used is high, it is more interesting to stack tile permanent magnets axially magnetized. On the other hand, when the number of tile permanent magnets used is low, it is more interesting to stack tile permanent magnets radially magnetized. Furthemore, tile permanent magnets tangentially magnetized can also be a good compromise whatever the number of tile permanent magnets used.

Figures 9 and 10 present elements of information about how to optimize cylindrical magnetic couplings with radial, axial or tangential polarizations. In short, the air gap must always be the smallest and the magnet thickness should be the greatest. However, the cost and the weight of the magnet structure must also be taken into account.
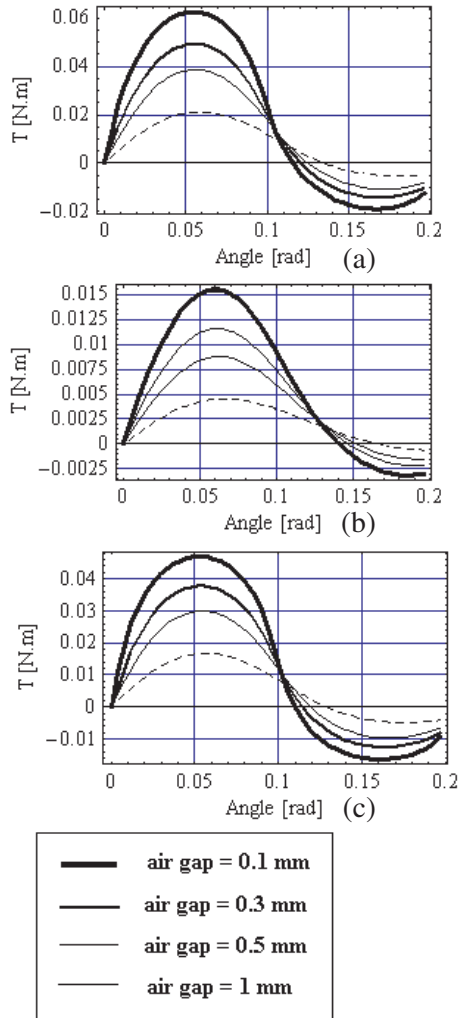
Figure 9. Representation of the torque transmitted between two rotors with a cylindrical air gap with tile permanent magnets radially (a) axially (b) and tangentially (c) magnetized with four air gaps (0.1 mm, 0.3 mm, 0.5 mm, 1 mm); we take the following dimensions: $r_2 - r_1 = 0.003$ m, $r_4 - r_3 = 0.003$ m, $z_1 = 0$ m, $z_2 = 0.003$ m, $z_3 = 0$ m, $z_4 = 0.003$ m, $J_1 = J_2 = 1$ T, $\theta_4 - \theta_3 = \theta_2 - \theta_1 = \frac{\pi}{32}$.
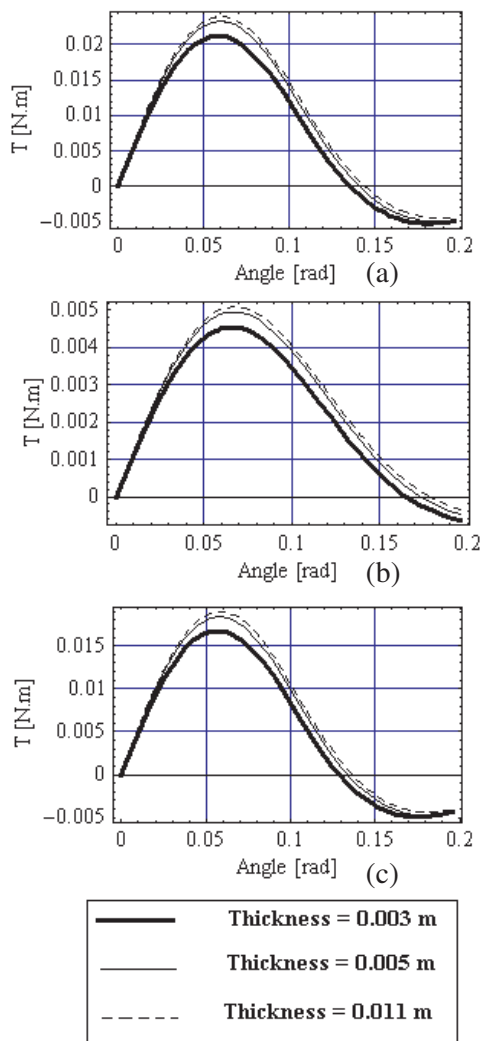
Figure 10. Representation of the torque transmitted between two rotors with a cylindrical air gap with tile permanent magnets radially (a), axially (b) and tangentially (c) magnetized with three magnet thicknesses (0.003 m, 0.005 m, 0.011 m); we take the following dimensions: $r_2 = 0.024$ m, $r_3 = 0.025$ m, $z_1 = 0$ m, $z_2 = 0.003$m, $z_3 = 0$ m, $z_4 = 0.003$ m, $J_1 = J_2 = 1\,T$, $\theta_4 - \theta_3 = \theta_2 - \theta_1 = \frac{\pi}{32}$.

7. CONCLUSION

This paper has presented a synthesis of magnetic couplings made of tile permanent magnets radially, tangentially or axially magnetized. First, we have presented new semi-analytical expressions of the torque transmitted between two tile permanent magnets tangentially and axially magnetized. Such a three-dimensional approach allows us to compare several configurations made of tile permanent magnets radially, tangentially or axially magnetized. All the calculations have been carried out without any simplifying assumptions. Therefore, these expressions are accurate whatever the tile permanent magnet dimensions. Then, we have proposed to compare magnetic couplings using cylindrical air gaps and magnetic couplings using plane air gaps. For the ones using cylindrical air gaps, it is always more interesting to use tile permanent magnets radially magnetized. For the couplings using plane air gaps, the most interesting polarization depends greatly on the number of tile permanent magnets used. However, when the angular width of the tile permanent magnet is greater than $\frac{Pi}{4}$, the axial polarization is the most interesting in the case of plane air gaps. Eventually, these studies illustrate the interest of the torque expressions presented when it comes to design choices and device optimization.

REFERENCES

1. Baran, W. and M. Knorr, "Synchronous couplings with sm co5 magnets," *2nd Int. Workshop on Rare-earth Cobalt Permanent Magnets and Their Applications*, 140–151, Dayton, Ohio, USA, 1976.

2. Yonnet, J. P., "Permanent magnet bearings and couplings," *IEEE Trans. Magn.*, Vol. 17, No. 1, 1169–1173, 1981.

3. Yonnet, J. P., S. Hemmerlin, E. Rulliere, and G. Lemarquand, "Analytical calculation of permanent magnet couplings," *IEEE Trans. Magn.*, Vol. 29, No. 6, 2932–2934, 1993.

4. Furlani, E. P., "Formulas for the force and torque of axial couplings," *IEEE Trans. Magn.*, Vol. 29, No. 5, 2295–2301, 1993.

5. Nagrial, M. M., "Design optimization of magnetic couplings using high energy magnets," *Electric Power Components and Systems*, Vol. 21, No. 1, 115–126, 1993.

6. Furlani, E. P. and T. S. Lewis, "A two-dimensional model for the torque of radial couplings," *Int J. Appl. Elec. Mech.*, Vol. 6, No. 3, 187–196, 1995.

7. Furlani, E. P., R. Wang, and H. Kusnadi, "A three-dimensonal model for computing the torque of radial couplings," *IEEE Trans. Magn.*, Vol. 31, No. 5, 2522–2526, 1995.

8. Furlani, E. P., "Analysis and optimization of synchronous magnetic couplings," *Journal of Applied Physics*, Vol. 79, No. 8, 4692–4694, 1996.

9. Elies, P. and G. Lemarquand, "Analytical optimization of the torque of a permanent-magnet coaxial synchronous coupling," *IEEE Trans. Magn.*, Vol. 34, No. 4, 2267–2273, 1998.

10. Li, Y., J. Zou, and Y. Lu, "Optimum design of magnet shape in permanent-magnet synchronous motors," *IEEE Trans. Magn.*, Vol. 39, No. 11, 3523–4205, 2003.

11. Ravaud, R., G. Lemarquand, V. Lemarquand, and C. Depollier, "Torque in permanent magnet couplings: Comparison of uniform and radial magnetization," *Journal of Applied Physics*, Vol. 105, No. 5, 2009.

12. Selvaggi, J. P., S. Salon, O. M. Kwon, and M. V. K. Chari, "Calculating the external magnetic field from permanent magnets in permanent-magnet motors — An alternative method," *IEEE Trans. Magn.*, Vol. 40, No. 5, 3278–3285, 2004.

13. Kwon, O. M., C. Surussavadee, M. V. K. Chari, S. Salon, and K. S. Vasubramaniam, "Analysis of the far field of permanent magnet motors and effects of geometric asymmetries and unbalance in magnet design," *IEEE Trans. Magn.*, Vol. 40, No. 3, 435–442, 2004.

14. Perigo, E., R. Faria, and C. Motta, "General expressions for the magnetic flux density produced by axially magnetized toroidal permanent magnets," *IEEE Trans. Magn.*, Vol. 43, No. 10, 3826–3832, 2007.

15. Jian, L. and K. T. Chau, "Analytical calculation of magnetic field distribution in coaxial magnetic gears," *Progress In Electromagnetics Research*, PIER 92, 1–16, 2009.

16. Babic, S. I., C. Akyel, and M. M. Gavrilovic, "Calculation improvement of 3D linear magnetostatic field based on fictitious magnetic surface charge," *IEEE Trans. Magn.*, Vol. 36, No. 5, 3125–3127, 2000.

17. Yonnet, J. P., *Rare-earth Iron Permanent Magnets*, Ch. Magnetomechanical Devices, Oxford Science Publications, 1996.

18. Huang, S. M. and C. K. Sung, "Analytical analysis of magnetic couplings with parallelepiped magnets," *Journal of Magnetism and Magnetic Materials*, Vol. 239, 614–616, 2002.

19. Ravaud, R., G. Lemarquand, V. Lemarquand, and C. Depollier, "The three exact components of the magnetic field created by a radially magnetized tile permanent magnet," *Progress In Electromagnetics Research*, PIER 88, 307–319, 2008.

20. Ravaud, R., G. Lemarquand, V. Lemarquand, and C. Depollier, "Permanent magnet couplings: Field and torque three-dimensional expressions based on the coulombian model," *IEEE Trans. Magn.*, Vol. 45, No. 4, 1950–1958, 2009.

21. Ravaud, R. and G. Lemarquand, "Analytical expression of the magnetic field created by tile permanent magnets tangentially magnetized and radial currents in massive disks," *Progress In Electromagnetics Research B*, Vol. 13, 309–328, 2009.

22. Ravaud, R., G. Lemarquand, V. Lemarquand, and C. Depollier, "Magnetic field produced by a tile permanent magnet whose polarization is both uniform and tangential," *Progress In Electromagnetics Research B*, Vol. 13, 1–20, 2009.

23. Babic, S. I. and C. Akyel, "Improvement in the analytical calculation of the magnetic field produced by permanent magnet rings," *Progress In Electromagnetics Research C*, Vol. 5, 71–82, 2008.

24. Ravaud, R., G. Lemarquand, V. Lemarquand, and C. Depollier, "Discussion about the analytical calculation of the magnetic field created by permanent magnets," *Progress In Electromagnetics Research B*, Vol. 11, 281–297, 2009.

25. Furlani, E. P., S. Reznik, and A. Kroll, "A three-dimensonal field solution for radially polarized cylinders," *IEEE Trans. Magn.*, Vol. 31, No. 1, 844–851, 1995.

26. Furlani, E. P., "Field analysis and optimization of ndfeb axial field permanent magnet motors," *IEEE Trans. Magn.*, Vol. 33, No. 5, 3883–3885, 1997.

27. Akoun, G. and J. P. Yonnet, "3D analytical calculation of the forces exerted between two cuboidal magnets," *IEEE Trans. Magn.*, Vol. 20, No. 5, 1962–1964, 1984.

28. Elies, P. and G. Lemarquand, "Analytical study of radial stability of permanent magnet synchronous couplings," *IEEE Trans. Magn.*, Vol. 35, No. 4, 2133–2136, 1999.

29. Yao, Y. D., D. R. Huang, C. C. Hsieh, D. Y. Chiang, S. J. Wang, and T. F. Ying, "The radial magnetic coupling studies of perpendicular magnetic gears," *IEEE Trans. Magn.*, Vol. 32, No. 5, 5061–5063, 1996.

30. Furlani, E. P., "A two-dimensional analysis for the coupling of

magnetic gears," *IEEE Trans. Magn.*, Vol. 33, No. 3, 2317–2321, 1997.

31. Lemarquand, V., J. F. Charpentier, and G. Lemarquand, "Nonsinusoidal torque of permanent-magnet couplings," *IEEE Trans. Magn.*, Vol. 35, No. 5, 4200–4205, 1999.

32. Charpentier, J. F. and G. Lemarquand, "Calculation of ironless permanent magnet coupling using semi-numerical magnetic pole theory method," *COMPEL*, Vol. 20, No. 1, 72–89, 2001.

33. Charpentier, J. F. and G. Lemarquand, "Optimal design of cylindrical air-gap synchronous permanent magnet couplings," *IEEE Trans. Magn.*, Vol. 35, No. 2, 1037–104, 1999.

34. Charpentier, J. F. and G. Lemarquand, "Optimization of unconventional p.m. couplings," *IEEE Trans. Magn.*, Vol. 38, No. 2, 1093–1096, 2002.

35. Babic, S. I. and C. Akyel, "Magnetic force calculation between thin coaxial circular coils in air," *IEEE Trans. Magn.*, Vol. 44, No. 4, 445–452, 2008.

36. Akyel, C., S. I. Babic, and M. M. Mahmoudi, "Mutual inductance calculation for non-coaxial circular air coils with parallel axes," *Progress In Electromagnetics Research*, PIER 91, 287–301, 2009.

37. Wang, R., E. P. Furlani, and Z. J. Cendes, "Design and analysis of a permanent-magnet axial coupling using 3D finite element field computation," *IEEE Trans. Magn.*, Vol. 30, No. 4, 2292–2295, 1994.

38. Azzerboni, B., G. A. Saraceno, and E. Cardelli, "Threedimensional calculation of the magnetic field created by currentcarrying massive disks," *IEEE Trans. Magn.*, Vol. 34, No. 5, 2601–2604, 1998.

39. Chau, K. T., D. Zhang, J. Z. Jiang, and L. Jian, "Transient analysis of coaxial magnetic gears using finite element comodeling," *Journal of Applied Physics*, Vol. 103, No. 7, 1–3, 2008.

40. Bancel, F. and G. Lemarquand, "Three-dimensional analytical optimization of permanent magnets alternated structure," *IEEE Trans. Magn.*, Vol. 34, No. 1, 242–247, 1998.